Anomalous Magnetotransport Properties of $R_2Mo_2O_7$ near the Magnetic Phase Boundary

T. Katsufuji,* H. Y. Hwang, and S-W. Cheong†

Bell Laboratories, Lucent Technologies, 600 Mountain Avenue, Murray Hill, New Jersey 07974

(Received 23 July 1999)

The magnetic and transport properties of pyrochlore $R_2Mo_2O_7$ have been studied with variation of the rare earth (R). The change of the mean ionic radius of R, which induces change of the lattice structure, determines the magnetic ground state (ferromagnetic or spin glass), and the magnetic phase boundary is correlated with the metal-insulator crossover. Furthermore, we found enhanced magnetoresistance and unusual residual anomalous Hall effect at low temperatures near the phase boundary, which can be attributed to the coexistence of both phases.

PACS numbers: 75.70.Pa, 71.30.+h, 75.50.Cc, 75.50.Lk

Recent studies of perovskite manganites [1] have revealed strong coupling between charge and spin degrees of freedom, as well as orbital degrees of freedom associated with Jahn-Teller distortion. Because of this intricate interplay, various competing ground states appear in mixed-valent manganites as a function of carrier concentration and also chemical pressure. It has been realized that extraordinary transport properties such as colossal magnetoresistance (MR) effects in manganites are associated with the proximity to phase boundaries between competing ground states. For example, MR is drastically enhanced when the system is close to the phase boundary between ferromagnetic (FM) metallic state and the charge-ordered (CO) insulating state.

Most FM compounds outside of the manganites do not show a clear correlation between FM and metallicity. With the variation of chemical pressure, many systems remain metallic even though the magnetic properties change drastically. For example, $SrRuO_3$ is FM and metallic, but replacing Sr by the smaller Ca ion leads to an antiferromagnetic (AF), but still metallic ground state [2]. $Co(S,Se)_2$ is another example: CoS_2 is FM and metallic, but $CoSe_2$ with large Se ions is an AF metal [3]. Pyrochlore $R_2Mo_2O_7$, with R = rare earth, is a series of compounds which might exhibit an interesting correlation between FM and metallicity [4]. In this series, those with R = Nd, Sm, and Gd are known to show ferromagnetic (FM) metallic behavior, whereas those with R = Tb and Dy, and smaller rare earths show a spin-glass (SG) behavior with fairly high resistivity. Mo $4d$ electrons are believed to play the principal role for the conduction and ferromagnetism, though the possible role of large 4f spins in R has not been clarified. The spin-glass phase of this series originates from the geometrical frustration of antiferromagnetically coupled spins [5], and thus this system gives a unique opportunity to study the transition from a geometrically frustrated Mott insulator to a ferromagnetic metal.

In this work, we have synthesized high-quality $R_2Mo_2O_7$ with various mixtures of R, and have studied magnetic and transport properties in detail. We found that the mean ionic radius of R, $\langle r_R \rangle$, determines the magnetic ground state, i.e., ferromagnetic or spin-glass states, and that the magnetic phase boundary correlates with the metal-insulator crossover. We also found that the ferromagnetic state near the phase boundary shows an additional spin-glass character, which results in various anomalies in magnetotransport properties.

Samples investigated in this work are polycrystals of $R_2Mo_2O_7$ with the mixture of (Gd, Dy), (Sm, Dy), (Gd, Tb), (Sm, Tb), and (Nd, Tb). First, MoO_2 was prepared by reacting Mo and MoO_3 in a sealed quartz tube (800 °C), and then $R_2Mo_2O_7$ was synthesized by reacting R_2O_3 and MoO_2 under Ar atmosphere (1350 °C). X-ray powder diffraction measurement (with Cu radiation) indicates that all samples are single phase with cubic symmetry. Lattice constants of all specimens were obtained by analyzing the x-ray diffraction peaks for $10° < 2\theta < 70°$. We also checked the Mo valence by thermogravimetric analysis, and found that the samples are stoichiometric within the resolution of 1% in valence. Magnetization measurements were done by using a quantum design SQUID magnetometer. For resistivity and MR measurements, we employed the conventional four-probe technique. Hall resistivity was measured by sweeping the magnetic field (perpendicular to the current) from -8 to 8 T and measuring the voltage perpendicular to the current and magnetic field. The offset due to MR was subtracted by taking the difference of the Hall voltage at H and $-H$.

Figure 1(a) shows the magnetization under 100 G as a function of temperature (T) for the (Gd, Dy) series (solid lines), as well as for the (R, Tb) series with $x = 0.5$ (dashed lines). The magnetization of $Gd_2Mo_2O_7$ ($x = 0$) sharply increases at about 70 K, which is typical behavior for a FM transition. The Curie temperature (T_C) decreases with increasing Dy concentration (x), and the samples for $x \geq 0.4$ do not show such an increase in magnetization. For $x \geq 0.4$, however, the magnetization curve shows significant difference between field cooling and zero-field cooling run below ~25 K, indicating a SG transition [4]. In the (R, Tb) series, T_C also decreases with decreasing $\langle r_R \rangle$ from Nd to Gd.

Those results of magnetization measurements are summarized in Fig. 2(a) as a function of $\langle r_R \rangle$ [6]. It should

 0031-9007/00/84(9)/1998(4)$15.00

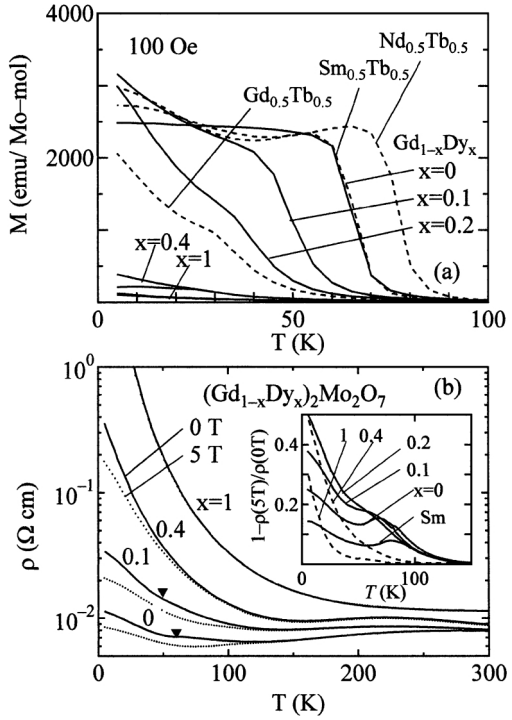

FIG. 1. (a) Magnetization under 100 G vs temperature for $(Gd_{1-x}Dy_x)_2Mo_2O_7$ (solid lines) and for $(R_{0.5}Tb_{0.5})_2Mo_2O_7$ with R = Nd, Sm, and Gd (dashed lines). (b) Resistivity vs temperature under 0 T (solid lines) and 5 T (dotted lines) for $(Gd_{1-x}Dy_x)_2Mo_2O_7$. The inset shows magnetoresistance $[1 - \rho(5\ \mathrm{T})/\rho(0\ \mathrm{T})]$ vs temperature for the (Gd,Dy) series as well as for $Sm_2Mo_2O_7$.

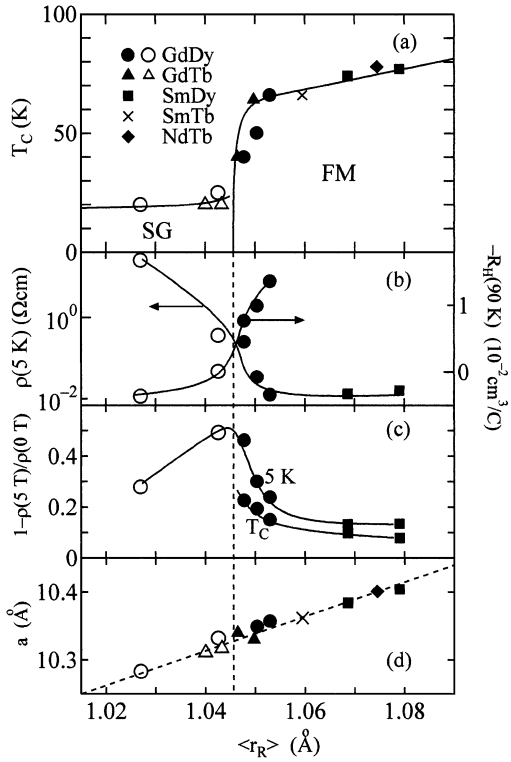

FIG. 2. (a) Phase diagram of $R_2Mo_2O_7$. Closed symbols show ferromagnetic transition temperatures and open symbols spin-glass transition temperatures. Circles correspond to $(Gd_{1-x}Dy_x)_2Mo_2O_7$ with $x = 0$, 0.1, 0.2, 0.4, and 1; squares to $(Sm_{1-x}Dy_x)_2Mo_2O_7$ with $x = 0$ and 0.2; triangles to $(Gd_{1-x}Tb_x)_2Mo_2O_7$ with $x = 0.25$, 0.5, 0.75, and 1; a cross to $(Sm_{1-x}Tb_x)_2Mo_2O_7$ with $x = 0.5$; and a rhombus to $(Nd_{1-x}Tb_x)_2Mo_2O_7$ with $x = 0.5$. (b) The values of resistivity at 5 K (left axis), and the values of $-R_H$ at 90 K (right axis). (c) Magnitude of magnetoresistance, $1 - \rho(5\ \mathrm{T})/\rho(0\ \mathrm{T})$, at 5 K and at T_C. (d) Lattice constants of the cubic structure. The x axis for all panels is the mean ionic radius of R.

be noted that the lattice constant changes almost linearly with $\langle r_R \rangle$, as shown in Fig. 2(d). If we assume that the Mo-O distance does not change for different R, a larger lattice constant in pyrochlore structure results in a larger Mo-O-Mo bond angle [7], and hence increased bandwidth. The FM and SG transition temperatures from magnetic data are summarized in Fig. 2(a) [8]. As clearly seen, all the data points for different combinations of R merge into a universal curve against $\langle r_R \rangle$, i.e., the FM state for a large R ($> R_c \sim 1.047$) and the SG state for a small R ($< R_c$). This result clearly excludes the possibility that the rare-earth moment dominates the magnetic ground state, but indicates that the structure is essential for the magnetic ground state.

Figure 1(b) shows the T dependence of resistivity without (solid lines) and with magnetic field (5 T, dotted lines). For the FM samples ($x = 0$ and 0.1), a small dip of resistivity is observed at T_C, shown by closed triangles. With increasing Dy concentration and the system becoming SG, resistivity becomes higher, particularly at low temperatures, suggesting a crossover from a metallic state to an insulating state. The residual resistivity at 5 K is plotted for the (Gd, Dy) and (Sm, Dy) series in Fig. 2(b) (left axis). Clear correlation between the magnetic phase boundary (shown by a dashed line) and the variation of the residual resistivity is observed, indicating that the FM-SG phase boundary is correlated with metal-insulator crossover in this molybdate system. This metal-insulator crossover can be explained qualitatively by the larger bandwidth for the samples with larger R and less distorted Mo-O-Mo bond. Thus, the correlation between FM and metallicity in this compound suggests that the FM interaction originates from the double-exchange mechanism, just like perovskite manganites [1]. It should be pointed out that the change of residual resistivity against $\langle r_R \rangle$ shown in Fig. 2(b) is not sharp enough to call it a metal-insulator transition. In other words, there is an intermediate range of $\langle r_R \rangle$, where the resistivity increases with decreasing temperature but remains finite at low temperatures, as exemplified in the main panel of Fig. 1(b) for $x = 0.1$ and 0.4. This may be related to the coexistence of two-component carriers as discussed below.

As seen in the main panel of Fig. 1(b), these molybdate compounds have a fairly large negative MR at low temperatures. The magnitude of MR, $1 - \rho(5\ \mathrm{T})/\rho(0\ \mathrm{T})$, is plotted as a function of T in the inset of Fig. 1(b). For

the samples in the FM regime (shown by solid lines), a peak at T_C is observed in the curve of MR vs T, which is typical of FM metals. Unlike normal FM metals, however, MR exists or is even increased at $T \ll T_C$ in these molybdates. Similar MR at low temperature (but without a peak at T_C) is also observed for the samples in the SG regime (shown by dashed lines). Focusing on the x dependence of MR at the lowest temperatures in the inset of Fig. 1(b), it has the maximum at $x = 0.2-0.4$. In other words, MR at the lowest temperature is enhanced near the FM-SG phase boundary, which is demonstrated in Fig. 2(c). This low-T MR is discussed later.

Hall measurements were done for $(Gd_{1-x}Dy_x)_2Mo_2O_7$, as shown in Fig. 3(a). Here, the Hall coefficient R_H is defined as the initial slope of the Hall resistivity (ρ_{xy}) vs magnetic field (H). R_H for the FM samples (shown by solid symbols) shows a sign change at ~130 K and its absolute value keeps on increasing with further decreasing T, whereas the samples in the SG regime (shown by open symbols) barely show such a sign change of the Hall coefficient, and it even increases further in the positive range with decreasing T for $x = 1$. The values of $-R_H$ at 90 K are plotted in Fig. 2(b) (right axis).

Figures 4(a) and 4(b) show the field dependence of the Hall resistivity (ρ_{xy}) for $Gd_2Mo_2O_7$. At high temperature, ρ_{xy} monotonically increases with field, but with decreasing T the slope decreases and becomes negative. Below 100 K, ρ_{xy} becomes nonlinear with the field, but the behavior changes again near 40 K. Above 40 K, ρ_{xy} goes to negative at low fields and then it increases linearly in high fields, whereas below 40 K both low-field and high-field parts behave in the opposite manner. In general, the Hall resistivity of the compounds that have localized moments is given by the sum of the ordinary and the anomalous term

$$\rho_{xy} = \mu_0 R_0 H + \mu_0 R_s M , \quad (1)$$

where R_0 and R_s are the ordinary and the anomalous Hall coefficients, respectively, μ_0 the vacuum permeability, and H the applied magnetic field. The field dependence of ρ_{xy} becomes nonlinear at low temperatures because of the saturation of M at high field. We fit the data of ρ_{xy} below 100 K to Eq. (1) by using experimentally measured $M(H,T)$. The values of the ordinary term, R_0, and the anomalous term, R_s, derived by the fitting are shown in Fig. 3(b) by crosses.

For the analysis of the high-temperature range (>100 K), where ρ_{xy} is difficult to decompose into the ordinary and the anomalous part experimentally, we assumed that (1) the anomalous part (R_s) is T independent, and (2) the ordinary part (R_0) has linear T dependence ($a + bT$) [10], and made the fitting of $R_H = R_0 + R_s\chi$ vs T. The dashed lines (the ordinary part and the anomalous part) as well as the solid line (calculated R_H) in Fig. 3(b) is the best fit using the experimentally measured

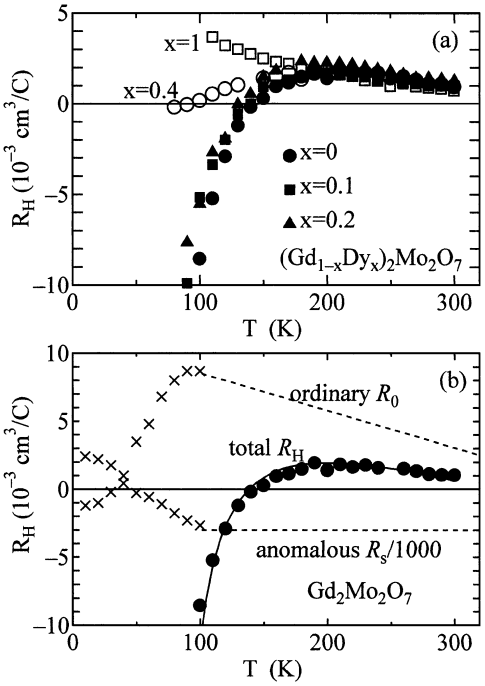

FIG. 3. (a) Hall coefficient vs temperature for $(Gd_{1-x}Dy_x)_2Mo_2O_7$. Closed symbols correspond to the samples in the FM regime ($x = 0$, 0.1, 0.2) whereas open symbols to those in the SG regime ($x = 0.4$, 1). (b) Crosses: ordinary (R_0) and anomalous (R_s) Hall coefficient derived from the fitting of ρ_{xy} shown in Fig. 4 for $Gd_2Mo_2O_7$. Closed circles: Hall coefficient $R_H = R_0 + R_s\chi$. Solid line: fitting curve for R_H. Dashed lines: ordinary and anomalous Hall coefficient estimated from the fitting shown by the solid line.

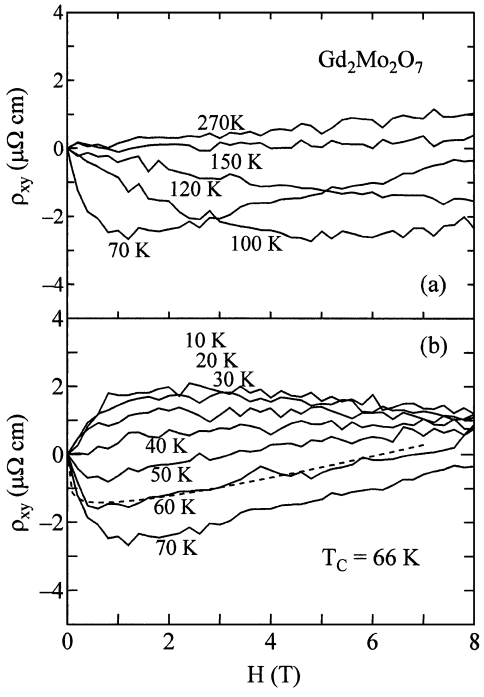

FIG. 4. Hall resistivity as a function of magnetic field for $Gd_2Mo_2O_7$. The dashed line shows the result of fitting to the data at 60 K.

susceptibility, $\chi(T)$, (at 1000 Oe). This result indicates that the zero crossing of R_H at ~130 K for the FM sample is due to the enhancement of the negative anomalous term, $R_s\chi$, associated with the increase of χ. We also calculated $R_H = R_0 + R_s\chi$ for other samples by using the same R_s and R_0 as those of $Gd_2Mo_2O_7$ ($x = 0$) but by using the experimentally measured $\chi(T)$ for each sample. We found that the calculated values are almost coincident with the experimental data for the FM sample, $x = 0.1$ and 0.2, but show clear deviation for the samples in the SG regime, $x = 0.4$ and 1, indicating that either R_0 or R_s (or more likely both) changes critically at the magnetic phase boundary.

What is unique to the Hall coefficient of this compound is the nonzero anomalous coefficient, R_s, for the FM sample at low temperature. For typical ferromagnetic metals, R_s approaches zero with T approaching zero, because the fluctuation of spins vanishes at low temperatures [9]. For pyrochlore molybdates, however, R_s crosses zero at ~40 K and changes its sign below, and does not vanish even at the lowest temperature, as shown in Fig. 3(b). It should be noted that the nonlinear field dependence of ρ_{xy} at 10 K shown in Fig. 4(b) is the direct consequence of this nonzero anomalous coefficient. This unusual behavior of the Hall coefficient appears to correlate with the nonzero MR at low temperatures shown in the inset of Fig. 1(b). One possible way to interpret these behaviors is to assume that the anomalous Hall coefficient as well as MR can be separated into two components, ferromagnetic and spin glass. In other words, the ferromagnetic state close to the magnetic phase boundary has an additional spin-glass character. For the anomalous Hall coefficient, the ferromagnetic component is negative, which becomes zero at the lowest temperature, whereas the spin-glass component is positive and nonzero at the lowest temperature. This assumption for the spin-glass component is consistent with the positive R_H at all temperatures for $Dy_2Mo_2O_7$ shown in Fig. 3(a). On the other hand, the ferromagnetic component of MR has the maximum near T_C and becomes zero at the lowest temperature, whereas the spin-glass component of MR has the maximum at the lowest temperature. This can explain the behavior of MR for $(Gd_{1-x}Dy_x)_2Mo_2O_7$ shown in the inset of Fig. 1(b). We point out that the crossoverlike behavior instead of a clear transition between metal and insulator under the variation of $\langle r_R \rangle$, as shown in Fig. 2(b), might also be related to such coexistence of two components.

It is not clear why the two components (FM and SG) exist near the phase boundary in these pyrochlore molybdates. One possible scenario is that two static phases (FM and SG) coexist in the real space, as proposed for perovskite manganites [11]. Another possible scenario is that the spin moments have both a statically ordered part contributing to the FM component, and a fluctuating part which freezes at low temperatures and contributes to the SG component. Since these molybdates have less Jahn-Teller distortion (due to their simple cubic structure) and thus their magnetic transition is less coupled with lattice distortions than in perovskite manganites, we speculate that the latter scenario is more realistic.

In summary, the magnetic ground states of $R_2Mo_2O_7$ is dominated by the change of lattice structure induced by the ionic radius of R, and metal-insulator crossover is correlated with the phase boundary between ferromagnetic and spin-glass states. The ferromagnetic state near the phase boundary has also a character of spin-glass state, which results in a large MR as well as a nonzero anomalous Hall coefficient at the lowest temperature.

We appreciate B. Batlogg for his help with measuring magnetization and T. Y. Koo for his help with analyzing x-ray data. We also thank C. M. Varma for useful discussions.

*Present address: Department of Advanced Materials Science, University of Tokyo, Tokyo 113-8656, Japan.
†Also Department of Physics and Astronomy, Rutgers University, Piscataway, NJ 08854.

[1] A. J. Millis, Nature (London) **392**, 147 (1998), and references therein.
[2] A. Kanbayasi, J. Phys. Soc. Jpn. **44**, 108 (1978).
[3] K. Adachi, M. Matsui, and M. Kawai, J. Phys. Soc. Jpn. **46**, 1474 (1979).
[4] N. Ali, M. P. Hill, S. Labroo, and J. E. Greedan, J. Solid State Chem. **83**, 178 (1989); J. E. Greedan, M. Sato, J. Ali, and W. R. Datars, J. Solid State Chem. **68**, 300 (1987).
[5] For example, see J. S. Gardner *et al.*, Phys. Rev. Lett. **83**, 211 (1999), and references therein.
[6] R. D. Shannon, Acta Cryst. A **32**, 751 (1976).
[7] This is experimentally confirmed for pyrochlore manganites. For example, see M. A. Subramanian *et al.*, J. Phys IV (France) **7**, C1-625 (1997).
[8] We define the Curie temperature as the peak position of dM/dT.
[9] P. Matl, N. P. Ong, Y. F. Yan, Y. Q. Li, D. Studebaker, T. Baum, and G. Doubinina, Phys. Rev. B **57**, 10 248 (1998), and references therein.
[10] For typical FM metals, the anomalous part (R_s) is usually T independent above T_C. [For example, see J. J. Rhyne *et al.*, Phys. Rev. **172**, 523 (1968).] On the other hand, T-independent ordinary part (R_0) together with the T-independent R_s could not fit the experimental data. Thus, the fitting function for the ordinary part, $R_0 = a + bT$, is the simplest functional form that can fit the data and can be connected continuously to the value below 100 K.
[11] M. Uehara, S. Mori, C. H. Chen, and S-W. Cheong, Nature (London) **399**, 560 (1999); A. Moreo, S. Yunoki, and E. Dagotto, Science **283**, 2034 (1999).